

UAV Fault-Tolerant Control by Combined \mathcal{L}_1 Adaptive Backstepping and Fault-dependent Control Allocation

Mikkel Eske Nørgaard Sørensen and Morten Breivik

Abstract—This paper presents an approach to obtain fault tolerance in the nonlinear longitudinal motion control of an aircraft. The approach uses an \mathcal{L}_1 adaptive backstepping controller and fault-dependent control allocation to obtain such tolerance. In the nominal fault-free case, only the elevator will be active. The \mathcal{L}_1 adaptive backstepping controller provides some robustness to the system by handling uncertainties, which is utilized for fault accommodation if a partial fault occurs. Also, control allocation is used to redistribute control to other available healthy actuators to make the system fault tolerant against more severe faults and even to a total loss of the elevator. Simulations have been conducted on a model of a Cessna 182 and show excellent results for both the nominal and faulty scenarios.

Index Terms—Longitudinal motion control, Fixed-wing UAV, Fault-tolerant control, \mathcal{L}_1 adaptive backstepping, Control allocation

I. INTRODUCTION

Critical safety issues must be considered when dealing with aircraft such as unmanned aerial vehicles (UAVs). In order to minimize risk, comprehensive checks are performed and meticulous maintenance is done regularly. Failures nevertheless occur, and actuator and control surfaces have particularly high criticality. Actuator redundancy can deal with some of the safety issues for small UAVs and fault-tolerant control (FTC) strategies can be employed to utilize redundancy in the actuators.

Many different control techniques have been applied for safety critical systems to tackle the problem of improving aircraft reliability. An overview of recent developments of FTC methods for aircraft is provided in [1], [2] and [3]. Specific fault diagnosis approaches are treated in [4], [5], [6] and [7] related to control surface fault diagnosis, and [8] for the airspeed sensor system. Two control techniques, namely sliding mode control (SMC) [9], [10] and the recent \mathcal{L}_1 adaptive control method [11], offer robust properties against matched uncertainties. The performance of SMC for attitude control for a fixed-wing UAV is investigated in [12]. The \mathcal{L}_1 adaptive control technique was shown in [13] to be robust against faulty actuators. The \mathcal{L}_1 adaptive backstepping control technique (L1-AB) was used in [14] as the pitch autopilot for an agile missile. The combination of L1-AB and control allocation (CA) was explored in [15]

M. Sørensen and M. Breivik are with the Centre for Autonomous Marine Operations and Systems (AMOS), Department of Engineering Cybernetics, Norwegian University of Science and Technology, NO-7491 Trondheim, Norway (mikkel.sorensen@itk.ntnu.no, morten.breivik@ieee.org)

to control an F16 in a fault-free case.

The CA approach can manage the redundancy of an over-actuated system [16]. CA is based on separating the control law from the control allocation task in a modular manner, where the control allocation task decides which actuator should receive a given control signal. This gives CA the possibility to be combined with any type of controller design. The combination is done by designing a controller to provide a “virtual high-level control” which is mapped to the actual control signals sent to the actuators. One of the benefits of using CA for systems where faults can occur, is that the controller structure does not have to be redesigned in the case of faults. It has the properties to deal directly with actuator faults without reconfiguring the controller since the allocation redistributes the control signal to healthy actuators.

Many small UAVs are not over-actuated and hence using CA to obtain redundancy in the actuators, as in [1] and [17], is not possible. Instead, this paper investigates CA of the forces and moments acting on the aircraft. The paper finds that it is not possible to maintain all forces and moments if a fault occurs since the aircraft has only one set of each control surface. The paper suggests how to prioritize forces and moments needed to stabilize a UAV where CA is combined with the L1-AB technique to obtain FTC for longitudinal UAV motion control [18].

The structure of the paper is as follows: A mathematical model and assumptions are presented in Section II; Section III deals with control allocation; Section IV presents control laws as applied to a fixed-wing UAV; Section V includes simulation results obtained from the combination of the control laws and the control allocation; and Section VI concludes the paper.

II. AIRCRAFT DYNAMICS

Longitudinal aircraft motion is considered, where the state vector $\mathbf{x}_{lon} \triangleq [\theta, Q, \alpha, V_t]^\top$ is defined, with the components pitch angle θ [rad], pitch rate Q [rad/s], angle of attack α [rad] and true airspeed V_t [m/s]. A controller is designed to control the angle of elevator deflection for the longitudinal nonlinear system. The dynamics of the longitudinal aircraft model can be stated as [19]:

$$\dot{\theta} = Q \quad (1)$$

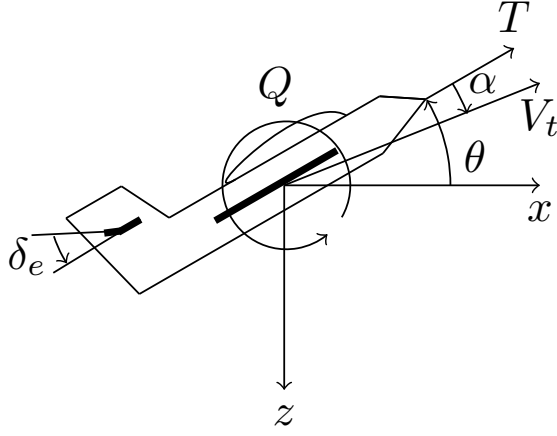


Fig. 1: Schematic of an aircraft

$$\begin{aligned}
I_y \dot{Q} &= \bar{m}(Q, \alpha, \dot{\alpha}, V_t, \delta_e) \\
&= \bar{q} \bar{S} \bar{c} \left(c_{m0} + c_{m\alpha}^* \alpha + c_{m\delta_e} \delta_e \right. \\
&\quad \left. + \frac{\bar{c}}{2V_t} (c_{m\dot{\alpha}}^* \dot{\alpha} + c_{mQ}^* Q) \right) \quad (2)
\end{aligned}$$

$$mV_t \dot{\alpha} = mg \cos(\theta - \alpha) - T \sin(\alpha) - L + mV_t Q \quad (3)$$

$$m\dot{V}_t = T \cos(\alpha) - D - mg \sin(\theta - \alpha), \quad (4)$$

where $m > 0$ [kg] represents the mass of the aircraft, $g = 9.81$ [m/s²] the acceleration of gravity, I_y the y-moment of inertia, $\bar{q} = \frac{1}{2}\rho V_t^2$ the dynamic pressure, \bar{S} wing area, \bar{c} the mean aerodynamic chord of the wing, ρ air density, δ_e deflection angle of the elevator [rad] and T engine thrust [N], which is modelled as

$$T = \frac{\eta \delta_t}{V_t}, \quad (5)$$

where η and δ_t are the propeller efficiency [%] and input power [W]. Furthermore, the relations between the drag D , lift L , side force Y , roll moment \bar{l} , pitch moment \bar{m} , yaw moment \bar{n} and the deflection of the control surfaces are [19]

$$D = \bar{q} \bar{S} [c_D(\mathbf{x}_{lon}, \delta_e) + \Delta_D(\mathbf{x}_{lon}, \delta_e)] \quad (6)$$

$$L = \bar{q} \bar{S} [c_L(\mathbf{x}_{lon}, \delta_e) + \Delta_L(\mathbf{x}_{lon}, \delta_e)] \quad (7)$$

$$Y = \bar{q} \bar{S} [c_Y(\mathbf{x}_{lat}, \delta_a, \delta_r) + \Delta_Y(\mathbf{x}_{lat}, \delta_a, \delta_r)] \quad (8)$$

$$\bar{l} = \bar{q} \bar{S} b [c_l(\mathbf{x}_{lat}, \delta_a, \delta_r) + \Delta_l(\mathbf{x}_{lat}, \delta_a, \delta_r)] \quad (9)$$

$$\bar{m} = \bar{q} \bar{S} \bar{c} [c_m(\mathbf{x}_{lon}, \delta_e) + \Delta_m(\mathbf{x}_{lon}, \delta_e)] \quad (10)$$

$$\bar{n} = \bar{q} \bar{S} b [c_n(\mathbf{x}_{lat}, \delta_a, \delta_r) + \Delta_n(\mathbf{x}_{lat}, \delta_a, \delta_r)], \quad (11)$$

where $\mathbf{x}_{lat} \triangleq [\phi, \psi, P, R, \beta]^T$ represents the lateral aircraft states, b wing span, δ_a deflection angle of the ailerons and δ_r the deflection angle of the rudder. The $\Delta_i(\mathbf{x}, \delta)$ terms, where the index i refers to forces and moments of (6)-(11), are unmodelled dynamics caused by uncertainty of the aerodynamic coefficients. It is assumed that $\Delta_i(\mathbf{x}, \delta)$ are unknown but bounded, as

$$\|\Delta_i(\mathbf{x}, \delta)\| \leq v_i(\mathbf{x}, \delta), \quad (12)$$

where $v_i(\mathbf{x}, \delta) > 0$ is a known function.

A. Assumptions

The control objective is to track a reference signal of the pitch angle θ_d , see Section IV. In order to design this controller, it is assumed that the true airspeed can be controlled separately and therefore can be neglected from the pitch controller design.

The angle of attack α is considered to be a function of time. Furthermore, the angle of attack and true airspeed need to meet the conditions:

$$|\alpha| \leq \alpha_{max} \quad (13)$$

$$|\dot{\alpha}| \leq \dot{\alpha}_{max} \quad (14)$$

$$0 < V_{t,min} \leq V_t \leq V_{t,max}. \quad (15)$$

It is assumed that uncertainties only exist in the coefficients of the pitch moment \bar{m} and that the aerodynamic coefficients c_{m0} and $c_{m\delta_e}$ are perfectly known. For the rest of the aerodynamic coefficients, the relationship between the real and considered coefficients is parametrised as

$$c_{m\alpha}^* = \sigma c_{m\alpha} \quad (16)$$

$$c_{m\dot{\alpha}}^* = \omega c_{m\dot{\alpha}} \quad (17)$$

$$c_{mQ}^* = \varphi c_{mQ}, \quad (18)$$

where c_{mi}^* represents the real coefficients, $\sigma \in \mathbb{R}^+$ is the uncertainty associated with the coefficient of pitch moment with respect to the angle of attack, $\omega \in \mathbb{R}^+$ is the uncertainty associated with the coefficient of pitch moment with respect to the derivative of angle of attack, and $\varphi \in \mathbb{R}^+$ is the uncertainty associated with the coefficient of pitch moment with respect to the pitch rate. Additionally, it is assumed that $\dot{\sigma} = 0$, $\dot{\omega} = 0$ and $\dot{\varphi} = 0$, i.e., that the uncertainties are constant or slowly varying relative to the aircraft dynamics.

Remark 1: In [21] and [22], it is shown through system identification that the aerodynamic coefficients c_{m0} and $c_{m\delta_e}$ are almost perfectly identified, which gives the basis for the assumption about these coefficients. In [23], uncertainty for the control signal and an external disturbance is also considered.

Using the assumptions together with (6)-(11), the longitudinal motion in (1)-(4) can be written as

$$\dot{\theta} = Q \quad (19)$$

$$\begin{aligned}
I_y \dot{Q} &= \bar{q} \bar{S} \bar{c} \left(c_{m0} + \sigma c_{m\alpha} \alpha + c_{m\delta_e} \delta_e \right. \\
&\quad \left. + \frac{\bar{c}}{2V_t} (\omega c_{m\dot{\alpha}} \dot{\alpha} + \varphi c_{mQ} Q) \right). \quad (20)
\end{aligned}$$

III. FAULT-DEPENDENT CONTROL ALLOCATION

For the analysis of the control allocation, it is assumed that only the elevator can be faulty. The partial loss of actuator effectiveness is a high-severity event and is commonly occurring in small aircraft. A decrease in the

effectiveness of an actuator is referred to as a *partial actuator loss* fault.

The fault on the actuator can be modelled as

$$\delta^a(t) = \mathbf{W}(t)\delta(t), \quad (21)$$

where $\delta^a \in \mathbb{R}^m$ is the actual control vector, $\delta \in \mathbb{R}^m$ is the control vector and $\mathbf{W}(t)$ represents the effectiveness of the actuators. The matrix $\mathbf{W}(t) \in \mathbb{R}^{3 \times 3}$ is defined as

$$\mathbf{W}(t) \triangleq \text{diag}(w_1(t), w_2(t), w_3(t)) = \mathbf{I} - \mathbf{K}(t), \quad (22)$$

where $\mathbf{I} \in \mathbb{R}^{3 \times 3}$ is the identity matrix and $\mathbf{K}(t) \in \mathbb{R}^{3 \times 3}$ is the multiplicative fault matrix which is defined for the aircraft as $\mathbf{K}(t) = \text{diag}(k_1(t), k_2(t), k_3(t))$ with $k_i(t) \in [0, 1]$, which is associated with the elevator, ailerons and rudder control surfaces. Here, $k_i = 0$ indicates that the i th control surface is in a fault-free condition, while $k_i = 1$ indicates that a total loss of effectiveness on the i th control surface has occurred.

Before the fault is introduced into the control allocation, it is necessary to determine the nominal angle of deflections on the control surfaces such that the aircraft can produce the commanded forces and moments from the controller in fault-free conditions, see Fig. 3. It should be noted that the control allocation does not take into account that there exists uncertainties in the pitch moment and therefore the following calculation only uses the nominal values of the aerodynamic coefficients.

Three equations are considered important to derive the nominal angle of deflections on the control surfaces for the considered forces and moments. These are the lift force, roll moment and yaw moment. The lift force is considered important since otherwise the aircraft is not able to stay airborne. It is desirable to stabilize the aircraft by keeping a certain moment when the aircraft is rolling or yawing, which is the reason for choosing the roll and yaw moment. Omitting the uncertainties $\Delta_i(\mathbf{x}, \delta)$, the lift force, roll moment and yaw moment in (7), (9) and (11) can be written as

$$L = \bar{q}\bar{S} \left(c_L(\mathbf{x}_{lon}) + \frac{\partial c_L}{\partial \delta_e} \delta_e \right) \quad (23)$$

$$\bar{l} = \bar{q}\bar{S}b \left(c_l(\mathbf{x}_{lat}) + \frac{\partial c_l}{\partial \delta_a} \delta_a + \frac{\partial c_l}{\partial \delta_r} \delta_r \right) \quad (24)$$

$$\bar{n} = \bar{q}\bar{S}b \left(c_n(\mathbf{x}_{lat}) + \frac{\partial c_n}{\partial \delta_a} \delta_a + \frac{\partial c_n}{\partial \delta_r} \delta_r \right). \quad (25)$$

The required angles of deflections on the control surfaces in the nominal cases are then determined to be:

$$\delta_{e,nom} = \frac{1}{\bar{q}\bar{S}\frac{\partial c_L}{\partial \delta_e}} (L - \bar{q}\bar{S}c_L(\mathbf{x}_{lon})), \quad (26)$$

$$\delta_{a,nom} = \frac{1}{\bar{q}\bar{S}b\frac{\partial c_l}{\partial \delta_a}} \left(\bar{l} - \bar{q}\bar{S}b \left(c_l(\mathbf{x}_{lat}) + \frac{\partial c_l}{\partial \delta_r} \delta_r \right) \right), \quad (27)$$

$$\delta_{r,nom} = \frac{1}{\bar{q}\bar{S}b \left(\frac{\partial c_l}{\partial \delta_a} \frac{\partial c_n}{\partial \delta_r} - \frac{\partial c_l}{\partial \delta_r} \frac{\partial c_n}{\partial \delta_a} \right)} \left(\frac{\partial c_n}{\partial \delta_a} (\bar{q}\bar{S}b c_l(\mathbf{x}_{lat}) - \bar{l}) + \frac{\partial c_l}{\partial \delta_a} (\bar{n} - \bar{q}\bar{S}b c_n(\mathbf{x}_{lat})) \right), \quad (28)$$

where it is assumed that the aerodynamic coefficients $\frac{\partial c_l}{\partial \delta_a}$, $\frac{\partial c_l}{\partial \delta_r}$, $\frac{\partial c_n}{\partial \delta_a}$ and $\frac{\partial c_n}{\partial \delta_r}$ are constant and nonzero around a stationary condition. This assumption is based on the measurements of various aircraft in a wind tunnel [20].

For the CA technique, the limitation on the angle of deflection on δ_i is considered as

$$\delta_{i,min} \leq \delta_i \leq \delta_{i,max}, \quad (29)$$

where $\delta_{i,min} < 0$ and $\delta_{i,max} > 0$, and where the index i refers to the elevator, ailerons or rudder, respectively.

A. Fault on the Elevator

A fault on the elevator is introduced to the system. To compensate for loss of effectiveness on the elevator δ_e when a partial-loss fault occurs, the angle of deflection for the reconfigured ailerons δ_a is recalculated for the drag force, lift force and pitch moment. Since it is the elevator that is faulty, it is desirable to control the pitch moment. This will of course affect the other inputs in the longitudinal system. The recalculation of the angle of deflection for the ailerons δ_a is a function of effectiveness on the elevator δ_e , where the goal is to maintain the pitch moment, which can be stated as

$$\delta_a = \frac{1}{\bar{q}\bar{S}\bar{c}\frac{\partial c_m}{\partial \delta_a}} \left(\bar{m} - \bar{q}\bar{S}\bar{c} \left(c_m(\mathbf{x}_{lon}) + \frac{\partial c_m}{\partial \delta_e} \delta_e w_1(t) \right) \right). \quad (30)$$

The fault-dependent control allocation approach is tested with the set point values from $\delta_{i,min}$ to $\delta_{i,max}$ for the elevator δ_e for the nominal case and with an effectiveness loss on the elevator. The inputs for the test are the nominal and not the actual angle of deflection on the elevator $\delta_{e,nom}$ and effectiveness of the elevator.

The calculated pitch moments for both the nominal case and the case where the elevator has lost 50%, 70%, 90% or 100% of its effectiveness are displayed as plots in Fig. 2. This figure also displays the difference between the nominal and faulty cases. From Fig. 2, it can be determined from which set point it is possible to maintain the same pitch moment by compensating the loss of the elevator with the ailerons. The span where the error is zero will decrease with the effectiveness of the elevator.

This allocation method using only the ailerons to compensate for the loss of effectiveness on the elevator is not the most effective solution to the allocation problem, but gives a description of the performance of the allocation by using only the ailerons if elevator fault has occurred.

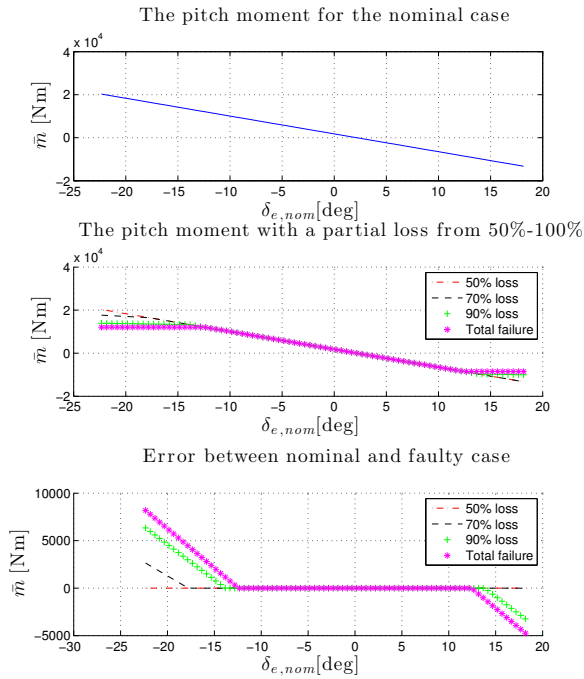


Fig. 2: Plots of the nominal, faulty and difference between the nominal and faulty cases for the pitch moment

Recalculating the angle of deflection for the elevator δ_e to compensate for some of the lost effectiveness before recalculating the angle of deflection on the ailerons δ_a shows less stress on the ailerons. This gives the opportunity to maintain the same forces and moments for a wider range and therefore is a better solution to the allocation problem. The recalculated angle of deflection on the elevator δ_e after computations is $\delta_e = \frac{\delta_{e,nom}}{w_1 + \varepsilon}$, where ε is a small positive constant. This new approach has been tested in the same manner as the former approach and gives a small improvement where the pitch moment of the normal and faulty cases are the same.

It is assumed in this paper that we have perfect knowledge of the faults, which is not the case in real-world systems. However, $\mathbf{W}(t)$ from (22) can be obtained by a separate fault identification scheme, see e.g. [1], [3], [8] and [24]. Also in order to compensate for the uncertainties that may occur in the relationship between the control surfaces and the actual forces and moments, L1-AB control is implemented. This will be discussed further in the following section.

IV. \mathcal{L}_1 ADAPTIVE BACKSTEPPING CONTROL

In this section, a step-by-step design procedure for the design of an \mathcal{L}_1 adaptive backstepping controller will be presented. It is assumed that both the pitch angle θ and pitch rate Q can be measured.

The control objective is to make $|\theta(t) - \theta_d(t)| \rightarrow 0$, where $\theta_d(t)$ is the desired pitch angle, which is \mathcal{C}^2 and

bounded. This reference signal is typically defined by a human or generated by a guidance system. For notational simplicity, the time t is omitted in the following.

The design of the \mathcal{L}_1 adaptive backstepping controller is divided into two stages. The first stage concerns the design of the adaptation laws and the second stage of the control law. The design is inspired by the approach in [14].

A. State Predictor and Adaptive Laws

First, we discuss the state predictor design. The prediction errors $\tilde{\theta}$ and \tilde{Q} are defined as

$$\tilde{\theta} \triangleq \hat{\theta} - \theta, \quad \tilde{Q} \triangleq \hat{Q} - Q, \quad (31)$$

where $\hat{\theta}$, \hat{Q} , θ and Q represent the estimated pitch angle, estimated pitch rate, real pitch angle and real pitch rate, respectively. The desired prediction error dynamics are chosen to be

$$\dot{\tilde{\theta}}_{ideal} = -L_1 \tilde{\theta}, \quad \dot{\tilde{Q}}_{ideal} = -L_2 \tilde{Q},$$

to ensure that their origins are exponentially stable, where the convergence rate is defined through the positive gains $L_1 > 0$ and $L_2 > 0$. From the latter, the state prediction dynamics are given as

$$\dot{\hat{\theta}} = -L_1 \tilde{\theta} + Q \quad (32)$$

$$\dot{\hat{Q}} = -L_2 \tilde{Q} + \frac{\bar{q}\bar{S}\bar{c}}{I_y} \left(c_{m0} + \hat{\sigma}c_{m\alpha}\alpha + c_{m\delta e}\delta_e + \frac{\bar{c}}{2V_t} (\hat{\omega}c_{m\dot{\alpha}}\dot{\alpha} + \hat{\varphi}c_{mQ}Q) \right), \quad (33)$$

where $\hat{\sigma}$, $\hat{\omega}$ and $\hat{\varphi}$ are the estimates of uncertainties on the aerodynamic coefficients. The design of adaptation laws for the uncertainties is based on Lyapunov stability analysis. Substituting (19), (20), (32) and (33) into (31), the prediction error dynamics become

$$\dot{\tilde{\theta}} = -L_1 \tilde{\theta} \quad (34)$$

$$\dot{\tilde{Q}} = -L_2 \tilde{Q} + \frac{\bar{q}\bar{S}\bar{c}}{I_y} \left(\tilde{\sigma}c_{m\alpha}\alpha + \frac{\bar{c}}{2V_t} (\tilde{\omega}c_{m\dot{\alpha}}\dot{\alpha} + \tilde{\varphi}c_{mQ}Q) \right). \quad (35)$$

Let's consider the positive definite Control Lyapunov Function (CLF)

$$V_{pred} = \frac{1}{2} \left(\frac{1}{\gamma_\sigma} \tilde{\sigma}^2 + \frac{1}{\gamma_\omega} \tilde{\omega}^2 + \frac{1}{\gamma_\varphi} \tilde{\varphi}^2 \right) + \frac{1}{2} \tilde{\theta}^2 + \frac{1}{2} \tilde{Q}^2, \quad (36)$$

where γ_σ , γ_ω and γ_φ are the adaptation gains for the estimation of σ , ω and φ , respectively. Taking the time

derivative of (36) yields

$$\begin{aligned}\dot{V}_{pred} &= \frac{1}{\gamma_\sigma} \tilde{\sigma} \dot{\sigma} + \frac{1}{\gamma_\omega} \tilde{\omega} \dot{\omega} + \frac{1}{\gamma_\varphi} \tilde{\varphi} \dot{\varphi} - L_1 \tilde{\theta}^2 - L_2 \tilde{Q}^2 \\ &+ \tilde{Q} \left(\frac{\bar{q} \bar{S} \bar{c}}{I_y} \left(\tilde{\sigma} c_{m\alpha} \alpha + \frac{\bar{c}}{2V_t} (\tilde{\omega} c_{m\dot{\alpha}} \dot{\alpha} \right. \right. \\ &\quad \left. \left. + \tilde{\varphi} c_{mQ} Q \right) \right) \\ &= -L_1 \tilde{\theta}^2 - L_2 \tilde{Q}^2 + \tilde{\sigma} \left(\frac{1}{\gamma_\sigma} \dot{\sigma} + \tilde{Q} \frac{\bar{q} \bar{S} \bar{c}}{I_y} c_{m\alpha} \alpha \right) \\ &+ \tilde{\omega} \left(\frac{1}{\gamma_\omega} \dot{\omega} + \tilde{Q} \frac{\bar{q} \bar{S} \bar{c}}{I_y} \frac{\bar{c}}{2V_t} c_{m\dot{\alpha}} \dot{\alpha} \right) \\ &+ \tilde{\varphi} \left(\frac{1}{\gamma_\varphi} \dot{\varphi} + \tilde{Q} \frac{\bar{q} \bar{S} \bar{c}}{I_y} \frac{\bar{c}}{2V_t} c_{mQ} Q \right). \quad (37)\end{aligned}$$

To eliminate the uncertainty terms $\tilde{\sigma}$, $\tilde{\omega}$ and $\tilde{\varphi}$, the adaptive update laws are then chosen as

$$\dot{\hat{\sigma}} = \gamma_\sigma \text{Proj} \left(\hat{\sigma}, -\tilde{Q} \frac{\bar{q} \bar{S} \bar{c}}{I_y} c_{m\alpha} \alpha \right) \quad (38)$$

$$\dot{\hat{\omega}} = \gamma_\omega \text{Proj} \left(\hat{\omega}, -\tilde{Q} \frac{\bar{q} \bar{S} \bar{c}}{I_y} \frac{\bar{c}}{2V_t} c_{m\dot{\alpha}} \dot{\alpha} \right) \quad (39)$$

$$\dot{\hat{\varphi}} = \gamma_\varphi \text{Proj} \left(\hat{\varphi}, -\tilde{Q} \frac{\bar{q} \bar{S} \bar{c}}{I_y} \frac{\bar{c}}{2V_t} c_{mQ} Q \right), \quad (40)$$

where $\text{Proj}(\cdot)$ denotes the projection operator [11]. Then (37) becomes

$$\dot{V}_{pred} = -L_1 \tilde{\theta}^2 - L_2 \tilde{Q}^2 \leq 0 \quad \forall \tilde{\theta}, \tilde{Q} \neq 0. \quad (41)$$

B. Control Law

We start by defining the error variables z_1 and z_2 as

$$z_1 \triangleq \theta - \theta_d \quad (42)$$

$$z_2 \triangleq Q - \alpha_1, \quad (43)$$

where α_1 is a stabilising function which is to be designed. Consider the positive definite CLF

$$V_{ctrl,1} = \frac{1}{2} z_1^2, \quad (44)$$

whose derivative with respect to time along the z_1 dynamics becomes

$$\begin{aligned}\dot{V}_{ctrl,1} &= z_1 \dot{z}_1 \\ &= z_1 (\dot{\theta} - \dot{\theta}_d) \\ &= z_1 (Q - Q_d).\end{aligned} \quad (45)$$

By substituting (43) into (45), the CLF becomes

$$\begin{aligned}\dot{V}_{ctrl,1} &= z_1 (z_2 + \alpha_1 - Q_d) \\ &= z_1 z_2 + z_1 (\alpha_1 - Q_d).\end{aligned}$$

The stabilising function can now be chosen as

$$\alpha_1 = -K_1 z_1 + Q_d, \quad (46)$$

where $K_1 > 0$, which gives

$$\dot{V}_{ctrl,1} = -K_1 z_1^2 + z_1 z_2. \quad (47)$$

The z_2 dynamics can be described as

$$\begin{aligned}\dot{z}_2 &= \dot{Q} - \dot{\alpha}_1 \\ &= \frac{\bar{q} \bar{S} \bar{c}}{I_y} \left(c_{m0} + \sigma c_{m\alpha} \alpha + c_{m\delta e} \delta_e \right. \\ &\quad \left. + \frac{\bar{c}}{2V_t} (\omega c_{m\dot{\alpha}} \dot{\alpha} + \varphi c_{mQ} Q) \right) - \dot{\alpha}_1.\end{aligned}$$

The CLF is then extended to

$$V_{ctrl,2} = \frac{1}{2} z_2^2 + V_{ctrl,1}, \quad (48)$$

such that it includes both z_1 and z_2 . The derivative of the new CLF is

$$\begin{aligned}\dot{V}_{ctrl,2} &= z_2 \dot{z}_2 + \dot{V}_{ctrl,1} \\ &= z_2 \left(\frac{\bar{q} \bar{S} \bar{c}}{I_y} \left(c_{m0} + \sigma c_{m\alpha} \alpha + c_{m\delta e} \delta_e \right. \right. \\ &\quad \left. \left. + \frac{\bar{c}}{2V_t} (\omega c_{m\dot{\alpha}} \dot{\alpha} + \varphi c_{mQ} Q) \right) - \dot{\alpha}_1 + z_1 \right) - K_1 z_1^2.\end{aligned}$$

The control law can now be chosen as

$$\begin{aligned}\delta_e &= -\frac{1}{c_{m\delta e}} \left(c_{m0} + \hat{\sigma} c_{m\alpha} \alpha + \frac{\bar{c}}{2V_t} (\hat{\omega} c_{m\dot{\alpha}} \dot{\alpha} \right. \\ &\quad \left. + \hat{\varphi} c_{mQ} Q) + \frac{I_y}{\bar{q} \bar{S} \bar{c}} (z_1 - \dot{\alpha}_1 + K_2 z_2) \right), \quad (49)\end{aligned}$$

where $K_2 > 0$, which leads to

$$\begin{aligned}\dot{V}_{ctrl,2} &= -K_2 z_2^2 - K_1 z_1^2 + z_2 \left(\frac{\bar{q} \bar{S} \bar{c}}{I_y} \left(\tilde{\sigma} c_{m\alpha} \alpha \right. \right. \\ &\quad \left. \left. + \frac{\bar{c}}{2V_t} (\tilde{\omega} c_{m\dot{\alpha}} \dot{\alpha} + \tilde{\varphi} c_{mQ} Q) \right) \right).\end{aligned} \quad (50)$$

For sufficiently large K_1 and K_2 , the system is stable since the estimates are bounded. $V_{ctrl,2}$ shows is input-to-state stable (ISS).

The adaptation of the uncertainties may contain high-frequency signals. To avoid introducing such frequencies into the control input, a lowpass filter is introduced to the control signals such that

$$\delta_{e,c} = C(s) \delta_e,$$

where

$$C(s) = \frac{k}{s+k},$$

is applied to the control signal and the gain $k > 0$ represents a design parameter of the lowpass filter.

V. SIMULATION RESULTS

This section starts by stating the aircraft model parameters, initial conditions and control parameters used in the Matlab simulations. Subsequently, the simulation results are shown and discussed.

A. Simulation Setup

The aircraft model of a Cessna 182 from [20] will be used to demonstrate the effectiveness and fault tolerance of the proposed technique. The aerodynamic constants for the reconfigured ailerons are chosen to be $c_{L\delta a} = 2c_{L\delta e}$ and $c_{m\delta a} = \frac{1}{2}c_{m\delta e}$. The initial conditions of the aircraft correspond to that it is flying straight and level, which means $\dot{Q} = \dot{\theta} = \dot{\alpha} = \dot{V}_t = 0$ and $\theta = \alpha = -0.0036$. The uncertainties are chosen as $\sigma = 0.7$, $\omega = 1.3$ and $\varphi = 0.9$, whose values are based on the result of system identification in [22].

Table I shows the parameters for the control law, state predictor and the adaptation laws. These were obtained after iterative tuning.

Control law		State predictor		Adaptation gains	
K_1 :	0.9	L_1 :	0.5	γ_σ :	4000
K_2 :	130	L_2 :	100	γ_ω :	4000
				γ_φ :	4000

TABLE I: Controller, state predictor and adaptation gains

A general schematic of the proposed actuator FTC technique is displayed in Fig. 3.

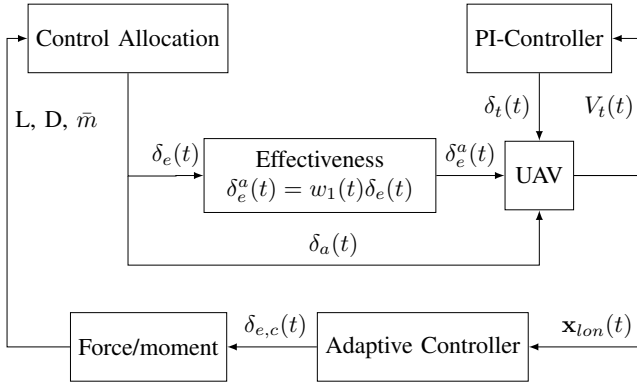
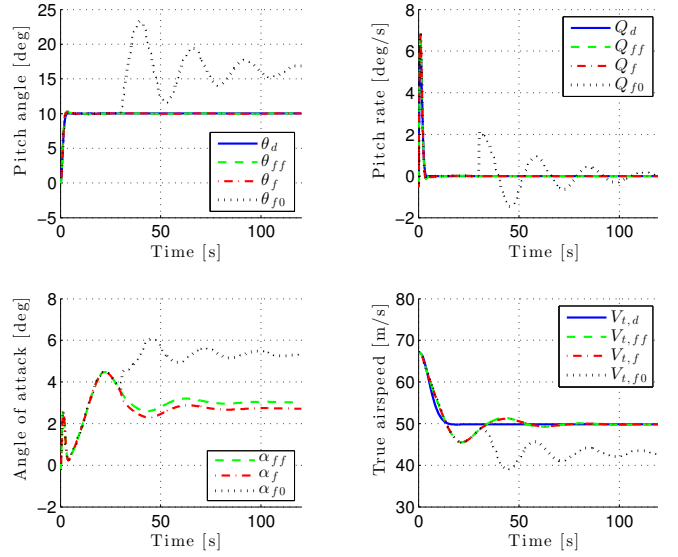


Fig. 3: Schematic of the actuator FTC implementation

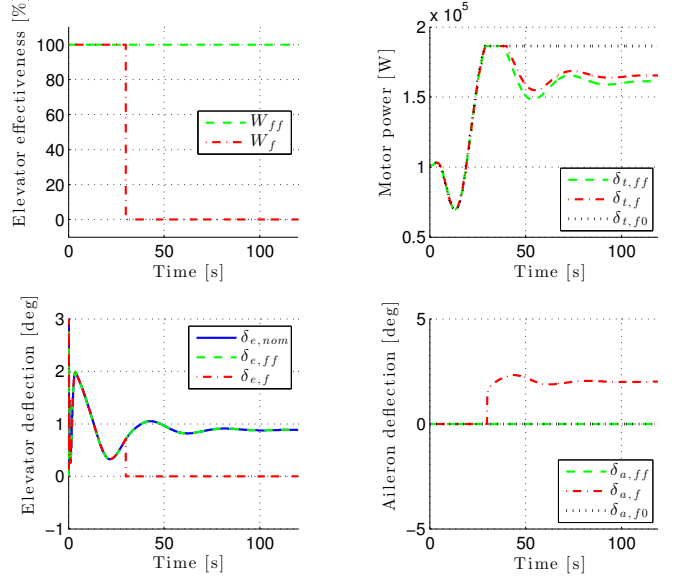
Here, the effectiveness matrix $\mathbf{W}(t)$ from (22) is assumed to be known. To control the airspeed during the simulation, a PI-controller has been implemented in a separate loop with gains $K_P = 0.3$ and $K_i = 1$.

B. Simulation Results

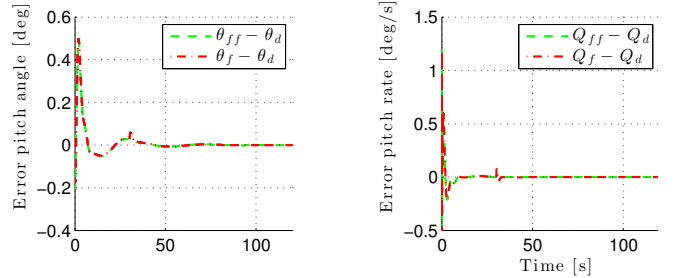
The simulation starts at an altitude and true airspeed of 1524 [m] and 67 [m/s], respectively. The aircraft starts to pitch up to 10 [deg] at 0 [s] and maintains such a pitch angle. It is also desirable to lower the true airspeed to the optimal climb speed of 50 [m/s]. The elevator actuator fault is set to occur at 30 [s]. In the following, the subscript ff and f refer to the fault-free and faulty system, respectively. Additionally, the system has been tested without having the FTC enabled, which is referred to $f0$ in the subscript. Fig. 4 illustrates the performance of the \mathcal{L}_1 adaptive backstepping controller for both a fault-free and faulty case.



(a) Aircraft states



(b) Actuator effectiveness and control inputs



(c) Aircraft pitch angle and rate errors

Fig. 4: Aircraft performance for both the fault-free and faulty cases

1) Fault-free case:

Fig. 4a shows a good pitch tracking performance, while the PI speed controller needs more time to reach its desired value. Since there is no fault, there is no control signal

distribution to the ailerons as shown in Fig. 4b. The tracking errors of Fig. 4c show that the aircraft tracks the pitch rate fast but need some more time for the pitch angle to settle.

2) 100% Effective Loss of the Elevator without FTC:

In the faulty case, the elevator goes to zero at 30 sec. The states in Fig. 4a show that the aircraft is no longer able to track the desired pitch angle and true airspeed after the fault has occurred. From Fig. 4b it can be concluded that this scenario has a high risk of going into an irreversible stall or spin. Since the elevator is stuck, there is no redundancy and the engine is already producing the maximum amount of power.

3) 100% Effective Loss of the Elevator with FTC:

Here, Fig. 4a shows only a change in angle of attack α when the fault occurs. By inspecting the inputs in Fig. 4b, the reason for this change in angle of attack is due to the amount of power the engine applies. Additionally, Fig. 4b shows that when the effect of the elevator is lost, the ailerons become active since the control signal is reallocated to them. Comparing the results in Fig. 4c of the fault-free and faulty cases shows no degradation in the performance when the elevator is faulty as long as the fault-tolerant controller is active.

VI. CONCLUSION

This paper has presented an approach to obtain fault tolerance in the nonlinear longitudinal motion of an aircraft. The proposed approach combines \mathcal{L}_1 adaptive backstepping control with fault-dependent control allocation, and allows the controller to operate in faulty conditions where the main actuator, which is the elevator, experiences a partial or total loss of its effectiveness. Since adaptive control can handle uncertainties, it provides some robustness to the system such that it can be controlled even if a partial fault has occurred. By adding control allocation that redistributes the control signal to a redundant control input, the system becomes fault tolerant against a total effective loss of the main actuator. Simulations conducted on a model of a Cessna 182 indicate excellent tracking performance for both the nominal and faulty cases when the FTC is active.

Future work includes a comparison of the performance between the proposed adaptive control algorithm and a robust control algorithm. Additionally, it is desirable to experimentally verify the results by implementing the methods on a hardware-in-the-loop simulator. To implement the proposed method in practice, it is also required to consider how to identify the fault and measure its magnitude, see e.g. [1], [3], [8] and [24].

ACKNOWLEDGMENT

This work was supported by the Research Council of Norway through the Centres of Excellence funding scheme, project number 223254.

REFERENCES

- [1] C. Edwards, T. Lombaerts, and H. Smaili, *Fault tolerant flight control: A benchmark challenge*. Springer, 2010.
- [2] A. Zolghadri, "Advanced model-based FDIR techniques for aerospace systems: Today challenges and opportunities," *Progress in Aerospace Sciences*, vol. 53, pp. 18–29, 2012.
- [3] P. Goupil, "Oscillatory failure case detection in the A380 electrical flight control system by analytical redundancy," *Control Engineering Practice*, vol. 18, no. 9, pp. 1110–1119, 2012.
- [4] E. Alcorta-Garcia, A. Zolghadri, and P. Goupil, "A nonlinear observer-based strategy for aircraft oscillatory failure detection: A380 case study," *IEEE Transactions on Aerospace and Electronic Systems*, vol. 47, no. 4, pp. 2792–2806, 2011.
- [5] S. Hansen and M. Blanke, "Control surface fault diagnosis with specified detection probability - Real event experiences," in *Proceedings of the International Conference on Unmanned Aircraft Systems (ICUAS)*, Atlanta, USA, 2013.
- [6] D. Efimov, J. Cieslak, A. Zolghadri, and D. Henry, "Actuator fault detection in aircraft systems: Oscillatory failure case study," *Annual Reviews in Control*, vol. 37, pp. 180–190, 2013.
- [7] M. Blanke and S. Hansen, "Towards self-tuning residual generators for UAV control surface fault diagnosis," in *Proceedings of the 2nd International Conference on Control and Fault-Tolerant Systems*, Nice, France, 2013.
- [8] S. Hansen and M. Blanke, "Diagnosis of airspeed measurement faults for unmanned aerial vehicles," *IEEE Transactions on Aerospace and Electronic Systems*, vol. 50, no. 1, pp. 224–239, 2014.
- [9] Y. Shtessel, *Sliding mode control and observation*. Birkhauser, 2013.
- [10] C. Edwards and S. K. Spurgeon, *Sliding mode control: Theory and applications*. Taylor and Francis Ltd, 1998.
- [11] N. Hovakimyan and C. Cao, \mathcal{L}_1 adaptive control theory: Guaranteed robustness with fast adaptation. SIAM, 2010.
- [12] T. Espinoza, A. Dzul, R. Lozano, and P. Parada, "Backstepping - sliding mode controllers applied to a fixed-wing UAV," in *Proceedings of the International Conference on Unmanned Aircraft Systems (ICUAS)*, Atlanta, USA, 2013.
- [13] V. V. Patel, K. A. Wise, N. Hovakimyan, C. Cao, and E. Lavretsky, " \mathcal{L}_1 adaptive controller for tailless unstable aircraft in the presence of unknown actuator failures," in *Proceedings of the AIAA Guidance, Navigation, and Control Conf.*, Hilton Head, South Carolina, USA, 2007.
- [14] C.-H. Lee, M.-J. Tahk, and B.-E. Jun, "Autopilot design for an agile missile using \mathcal{L}_1 adaptive backstepping control," in *Proceedings of the 28th Congress of the International Council of the Aeronautical Sciences*, Brisbane, Australia, 2012.
- [15] K. Liu, J. Zhu, and B. Yu, "Longitudinal controller design for a fighter aircraft using \mathcal{L}_1 adaptive backstepping," in *Proceedings of the World Congress on Intelligent Control and Automation*, Taipei, Taiwan, 2011.
- [16] J. D. Boskovic and R. K. Mehra, "Control allocation in overactuated aircraft under position and rate limiting," in *Proceedings of the American Control Conference*, Anchorage, USA, 2002.
- [17] M. T. Hamayun, H. Alwi, and C. Edwards, "An output integral sliding mode FTC scheme using control allocation," in *Proceedings of the 50th IEEE Conference on Decision and Control and European Control Conference (CDC-ECC)*, Orlando, USA, 2011.
- [18] G. J. J. Ducard, *Fault-tolerant flight control and guidance systems: Practical methods for small unmanned aerial vehicles*. Springer-Verlag, 2009.
- [19] B. L. Stevens and F. L. Lewis, *Aircraft control and simulation*. John Wiley and Sons, 2003.
- [20] J. Roskam, *Airplane flight dynamics and automatic flight controls*. DARcorporation, 2003.
- [21] D. Sansverinati, *Identification and fault diagnosis for autonomous aircraft*. MSc thesis. Dept. of Electrical Eng., Technical University of Denmark, 2010.
- [22] M. E. N. Sørensen, *Fault-Tolerant Control for Unmanned Aerial Vehicle*. MSc thesis. Dept. of Electrical Eng., Technical University of Denmark, 2014.
- [23] M. E. N. Sørensen and M. Breivik, "Comparing nonlinear adaptive motion controllers for marine surface vessels," in *Proceedings of the 10th IFAC Conference on Manoeuvring and Control of Marine Craft*, Copenhagen, Denmark, 2015.
- [24] M. Blanke, M. Kinnaert, J. Lunze, and M. Staroswiecki, *Diagnosis and fault-tolerant control*. Springer, second ed., 2006.